Fluid Solid Coupling Analysis of Large Underground Oil Storage Caverns in Containment of Groundwater

Yang Shang-Yang[1,2], Li Shu-Cai[1], Xue Yi-Guo[1] and Zhang Qing-Song[1]

[1.] *Geotechnical &Structural Engineering Research Center, Shandong University, Jinan, 250061, China*
[2.] *Department of Physics and Mathematics, Shandong Jiaotong University, Jinan, 250023, China*
yangsy@sdjtu.edu.cn,

Abstract

Triaxial compression tests had been performed to determine the properties of the rock mass around unlining underground crude oil a storage cavern which was the first one in China. The execution situation of the tunnel project and the seepage law of groundwater were taken into account. The stress and the seepage field around the tunnel in different working states were simulated by applying Comsol around a underground crude oil storage caverns. According to the test results, it was found that the excavation process may arise the local damage. The extension of the loose zone induced by excavation ranged from 0 to 15.6 m, depending on the buried depth of the caverns. According to numerical simulation results, the crown settlement and stress concentration was depended on the buried depth and the water pressure distribution after excavation of the main cavity. This research results can provide the reference for analysis on the stability of the underground cavities under low stress level and on the water sealed underground petroleum storage rock caverns.

Keyword: Triaxial compression tests; numerical simulation; crown settlement;fluid-solid coupling

1. Introduction

The water sealed underground petroleum storage rock caverns were commonly used as a way of oil reseres. This underground cavern should have two conditions: (1) seal, (2) having certain strength. The sealing was realized by the groundwater penetration into the hole. Underground structure must be built below the underground water level line in order to ensure that the groundwater pressure around the underground structure was greater than the pressure in the hole.

Robert(1995)[1] summarized the problems in the design and construction process of the unlining underground crude oil storage caverns, focusing on hydrogeology and surrounding rock stability.

Lee (1996, 1997) [2][3] made a detailed analysis in the design and construction process of the unlining underground crude oil storage caverns. Lee mainly analyzed the cavern working face and the blasting on deformation and stress of the surrounding rock. Gao-xiang[4] analyzed the development of artificial water curtain,basic principle, design and construction as well as running effect using artificial water curtain in unlined underground gas storage cavern engineering. Zhang-zhengang(2003,2006)[5] introduced the air condition of the sealing LPG underground storage and made 3D analysis on the propane storage of Shantou LPG underground storage. The research above effectively promoted the energy storage level of theory and technology in hard rock mass in China.

Numerical modeling had become increasingly popular for complex slope stability

analysis (Wei Chen *et al*. 2014, Kripamoy Sarkar *et al*. 2012, Tian-hong Yang *et al*. 2014, I. Shooshpasha *et al*. 2014, Ahmad Fahimifar *et al*. 2014, S. Srikrishnan *et al*. 2013)[6][7][8][9][10][11]. An extended three-dimensional model for standard tests was taken as the example with the purpose of the research on the stability of unsaturated soil slopes. Based on elasto-plastic constitutive model and strength criterion of unsaturated soils, the numerical simulations of slope stability were carried out(CHEN Yong *et al*., 2010)[12].

Kripamoy Sarkar *et al*. (2012) had carried out many field surveys and laboratory experiments to understand the geological detail. Three-dimensional slope stability studies were used to analyse the computed deformations and stress distribution of the slope. Finite difference method had been applied on the stability analysis of Amiyan slope.

Ebru Topsakal *et al*. (2014)[13] investigated the opening of boreholes with sampling and field testing, the geological mapping, laboratory studies, inclinometer measurements, and limit equilibrium analysis of the slope before and after remediation. The geological material of the landslide area was colluvium, mainly composed of sandy gravelly clay.

Lei Nie *et al*. (2014)[14], had studied the deformation characteristics and mechanism of the landslide of the West Open-Pit mine. The results showed deep rock mass sliding, large deformation of the partial surface of the landslide, and clear sliding surface dislocation characteristics.

The salty coefficients of landslide had been improved obviously with the help of stability analysis, which also could completely satisfy the standard requirement that the coefficients were no less than 1.25．Furthermore，based on the analysis of the load-unload response ratio model，the landslide was safe and stable by comprehensive treatment (XUE Xing-hua *et al*., 2011)[15].

In this paper, Triaxial compression tests had been performed to determine the properties of the rock mass around an unlining underground crude oil storage caverns which was the first one in China. Meanwhile, the strength and deformation characteristics of the caverns were analysed. This research results could provide the reference for analysis on the stability of the underground cavities under low stress and on the water sealed underground petroleum storage rock caverns.

2. Engineering Background

This project of the water sealed underground petroleum storage rock caverns was currently the first one ongoing large-scale underground crude oil reserve. The project site belonged to the hilly landscape. The mountain strike of the cavern site was about east-west. The elevation of ridge is 280~350m and the topographic slope is about $35\sim55^{\circ}$. The storage rock caverns strike was about north-west, 600m wide from east to west, 838m long from south to north, 300×10^4 m^3 designing capacity, and 50 years designing life. The underground storage had 9 holes which were set parallel to north-south direction. Each hole had 20m designing width, 30m height, and the straight wall round arched for the section shape.

3. Indoor Triaxial Compression Test

Triaxial compression tests had been performed to determine the properties of the rock mass around an unlining underground crude oil storage caverns. The sample granitic gneiss was taken from the engineering site which was in 180m burial depth. The sample was cut and polished into standard one whose density was 2.66×10^3 kg/m^3. The test equipment type RLW-500 rock triaxial apparatus was adopted (see figure 1). According burial depth, 5MPa was used as its confining pressure.

Figure 1. RLW-500 Rock Triaxial Apparatus for the Test

According to the test results, we gained the saturated specimen block density（ρ_D）, modulus of elasticity（E）, poisson's ratio（v）, cohesion（c）, friction angle（φ）(see Table 1)

Table 1. Physical and Mechanical Parameters of the Rock Mass Around the Caverns

category	ρ_D /(g·cm^{-3})	E /GPa	v	c / MPa	φ / (°)
granite	2.74	49.3	0.16	8.34	57.79

4. Seepage Formula

Fissuring seepage was the main seepage mode. Ignoring the permeability between the rocks, the fracture distribution was relatively dense. Because the representation elementary volume (REV) was small, we could use the contimuum as the approximation description. When the fractured rock mass was considered as equivalent continuum model [16], the partial differential equation of seepage was:

$$\frac{\partial}{\partial_x}\left(k_{xx}\frac{\partial\phi}{\partial x}+k_{yx}\frac{\partial\phi}{\partial y}+k_{zx}\frac{\partial\phi}{\partial z}\right)+ \tag{1}$$

$$\frac{\partial}{\partial_y}\left(k_{xy}\frac{\partial\phi}{\partial x}+k_{yy}\frac{\partial\phi}{\partial y}+k_{zy}\frac{\partial\phi}{\partial z}\right)+$$

$$\frac{\partial}{\partial_z}\left(k_{xz}\frac{\partial\phi}{\partial x}+k_{yz}\frac{\partial\phi}{\partial y}+k_{zz}\frac{\partial\phi}{\partial z}\right)+Q=S_s\frac{\partial\phi}{\partial t}$$

Coming down to：

$$K\nabla\phi=S_s\frac{\partial\phi}{\partial t} \tag{2}$$

Among ：

$$K=\begin{bmatrix}k_{xx}&k_{yx}&k_{zx}\\k_{xy}&k_{yy}&k_{zy}\\k_{xz}&k_{yz}&k_{zz}\end{bmatrix},\quad \nabla\phi=\left[\frac{\partial\phi}{\partial x},\frac{\partial\phi}{\partial y},\frac{\partial\phi}{\partial z}\right]^T \tag{3}$$

Coupled model
The seepage field mathematical model under the effect of stress field and the stress field mathematical model under the effect of seepage field could be used in coupled model.
(1). seepage field mathematical model under the effect of stress field

$$\begin{cases} \nabla(K\nabla\phi) + Q = \mu\dfrac{\partial\phi}{\partial t} & t \geq t_0, (x,y,z) \in \Omega \\[2mm] \phi(x,y,z,t_0) = \phi_0(x,y,z) & t = t_0, (x,y,z) \in \Omega \\[2mm] \phi(x,y,z,t) = \phi_1(x,y,z,t) & t \geq t_0, (x,y,z) \in \Gamma_1 \\[2mm] k_{xx}\cos(n,x)\dfrac{\partial\phi}{\partial x} + k_{yy}\cos(n,y)\dfrac{\partial\phi}{\partial y} \\[2mm] + k_{zz}\cos(n,z)\dfrac{\partial\phi}{\partial z} = q(x,y,z,t) & t \geq t_0, (x,y,z) \in \Gamma_1 \end{cases} \qquad (4)$$

(2). the stress field mathematical model under the effect of seepage field

$$\begin{cases} \sigma_{ij} + f_j = 0 & (x,y,z) \in \Omega \\[2mm] \varepsilon_{ij} = \dfrac{1}{2}(u_{i,j} + u_{j,i}) & (x,y,z) \in \Omega \\[2mm] \sigma_{ij}n_j = t_i(\phi) & (x,y,z) \in S_\sigma \\[2mm] u_i = \overline{u_i} & (x,y,z) \in S_u \\[2mm] \sigma_{ij} = \lambda\varepsilon_V\delta_{ij} + 2G\varepsilon_{ij} & (x,y,z) \in \Omega \end{cases} \qquad (5)$$

Among ：

Ω — the whole research area of the model ;

$\sigma_{ij} = \sigma_{ij}(x,y,z)$ — stress vector ;

$\varepsilon_{ij} = \varepsilon_{ij}(x,y,z)$ — strain vector ;

$u_i = u_i(x,y,z)$ — displacement field ;

ε_V — volumetric strain ;

λ — lame coefficient ;

G — shear modulus ;

δ_{ij} — kronecker symbol ;

f_j — body force ;

S_σ — surface force boundary ;

n_j — normal direction ;

$t_i(\phi)$ — surface force distribution ;

S_u — known displacement boundary ;

$\overline{u_i}$ — known displacement distribution

The matrix form solved by the finite element is

$$\{\sigma\} = [D]\left[\{\varepsilon\} + \{\Delta\varepsilon_V\}\right]$$

Among:

$\{\sigma\}$ — stress array of rock;

$\{\varepsilon\}$ — strain matrix without considering seepage pressure;

$\{\Delta\varepsilon_V\}$ — strain array of the rock displacement caused by seepage pressure;

$[D]$ — elastic matrix:

$$[D] = \frac{E(1-v)}{(1+v)(1-2v)} \begin{bmatrix} 1 & A & A & 0 & 0 & 0 \\ A & 1 & A & 0 & 0 & 0 \\ A & A & 1 & 0 & 0 & 0 \\ 0 & 0 & 0 & B & 0 & 0 \\ 0 & 0 & 0 & 0 & B & 0 \\ 0 & 0 & 0 & 0 & 0 & B \end{bmatrix} \tag{6}$$

Among which,

$$A = \frac{v}{1-v}; \quad B = \frac{1-2v}{2(1-v)}$$

By substitution of the body strain increment $\Delta\varepsilon_v$ obtained from $\{\sigma\}$ into formula (4), the changes of rock mass water pressure could be obtained. The stress field and seepage field coupling could be obtained by constantly iteration.

5. Calculation Example

In this paper, 4 nodes tetrahedral element was used in discretization research which had 300,000 elements (see Figure 2 and Figure 3). Boundary condition of seepage field: 0 pressure head for tunnel inside, no-flow boundaries for tunnel sides and bottom, 0 pore water pressure for top. Seepage initial condition: the initial pore water pressure being equal to hydrostatic pressure in rock before excavation. Stress boundary condition: horizontal restraint for model sides, vertical restraint for model bottom, free surface for model top and inner.
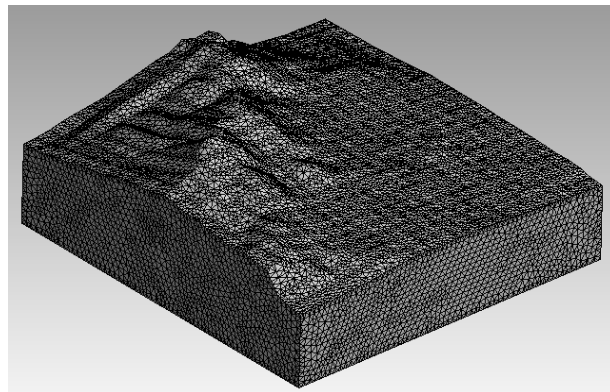

Figure 2. Finite Element Mesh for Rock Mass
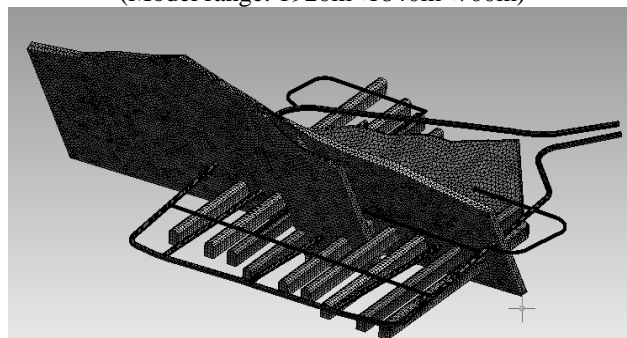
(Model range: 1920m×1840m×700m)

Figure 3. Finite Element Mesh for Caverns

6. Calculation Results and Analysis

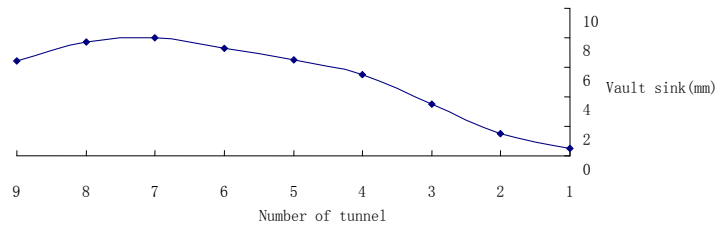### 6.1. Deformation and Stress Field

Figure 4. Vault Sink Curve after Excavation

The biggest change of displacement was found in 8# and 7# caverns according to the calculation result. Therefore, grouting treatment should be conducted on 8# and 7# caverns preventing large settlement. Meanwhile, support measures should be adopted in excavation.
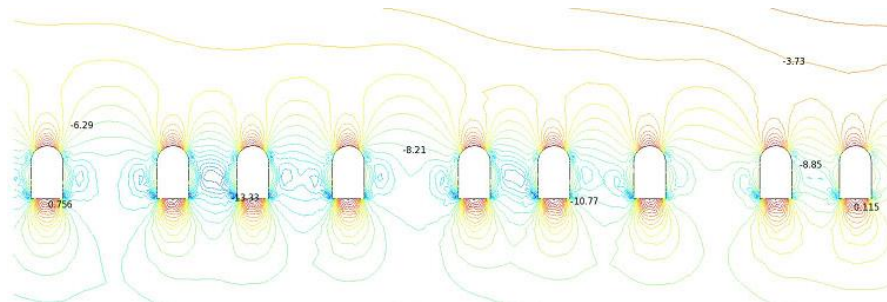

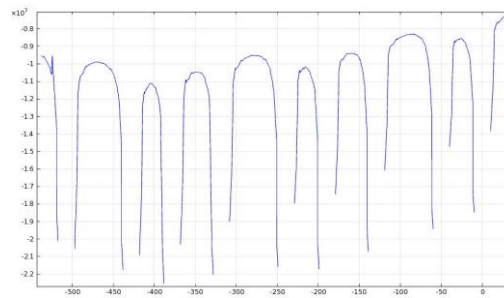**Figure 5. Contour Map for Vertical Direction after Excavation**

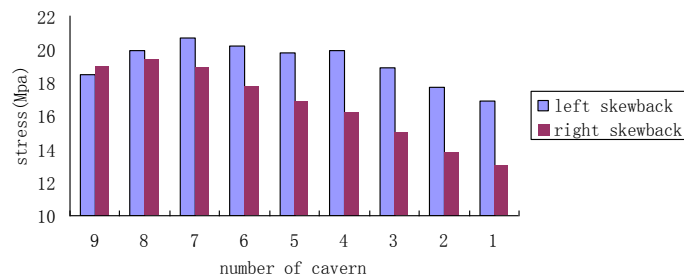**Figure 6. Change of Vertical Stress along the Horizontal Direction**

Figure 7. Comparison between Left Skewback and Right Skewback About Stress

Stress concentration could be obviously found at cavern skewback and spandrel after excavation (see Figure 5). In Figure 6, the curve interruption reflects the 9 main tunnels, and the curve endpoint reflects its vertical stress. Because there are 9 main tunnels, the 9 curve interruptions can be found in Figure 6. We could conclude that stress concentration was different between the left and right skewback of each cavern(see Figure 7). The left and right skewback stress of 8# and 9# cavern were much the same, about 20Mpa(see Figure 7), while, it was obviously different in the rest caverns. However, laws were consistent in every cavern(see Figure 7), in that, the stress of left skewback was bigger than the right one. So some pertinent treatment could be used in construction.
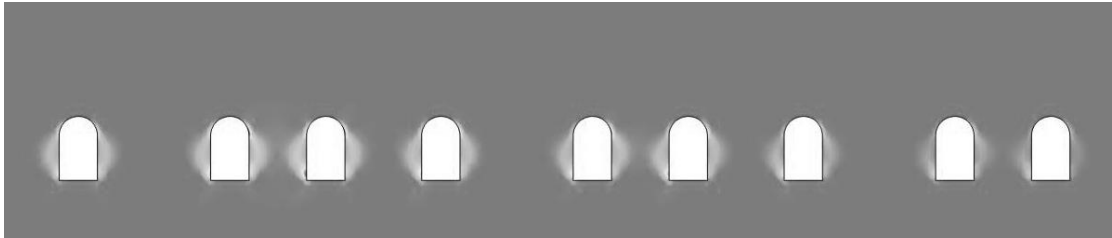

Figure 8. Equivalent Plastic Strain around the Caverns

Plastic zone transfixion was not found in calculation (see Figure 8), that was to say that the spacing of the caverns were reasonable. In 1# and 2 #，4# and 5#，7# and 8#, the range of plastic zone were obviously bigger than others, almost the samallest hole spacing.
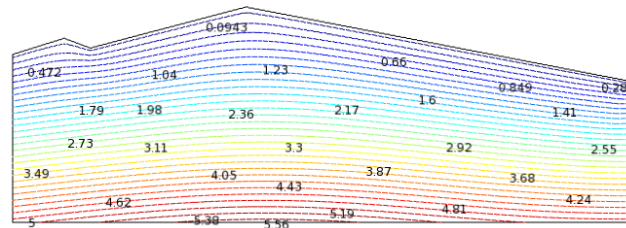
6.2. Seepage Field

Figure 9. Water Pressure Contour Map before Excavation (Mpa)

Pore water pressure changed according to the topographic trend before excavation (see Figure 9). In Figure 9, pore water pressure was related with the surface fluctuation situation. In the deeper burial depth zone of the same elevation, the initial ground stress and pore water pressures were bigger than others.
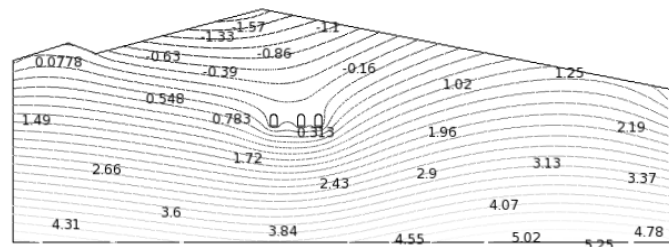

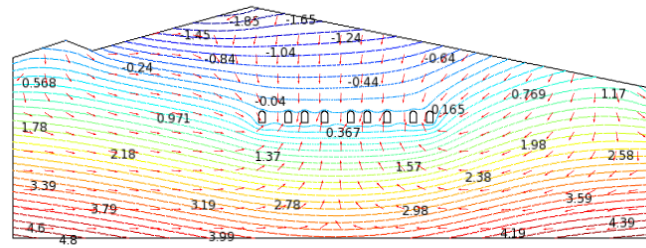**Figure 10. Pore Water Pressure after Excavating the Left 3 Tunnels**

Figure 11. Pore Water Pressure And Flow Vector after Excavation (Mpa)

Due to tunnel surrounding pressure imbalance after excavation which could be found in Figure 10, cavern inner pressure was less than the surrounding rock pressure. Therefor, we can find groundwater penetration into the hole, causing change of groundwater and forming cone of depression (see Figure 10).

In Figure 11, all the main tunnels were excavated, and we gained the flow vector map which was more intuitive to reflect the situation of groundwater seepage. We could clearly find groundwater permeability into the caverns in Figure 11. What was more, the denser the flow vector was the nearer the cavern was from, and the sparser the flow vector was the further the cavern was from. We could make the judgement that excavation had less influence on the water pressure far from the caverns.

7. Conclusion

(1) The biggest change of displacement was found in 8# and 7# caverns; therefore, grouting treatment should be conducted on 8# and 7# caverns preventing large settlement.

(2) Plastic zone transfixion was not found in calculation, that was to say, the spacing of the caverns were reasonable.

(3) Groundwater permeability into the caverns, the denser the flow vector was the nearer the cavern was from, and the sparser the flow vector was the further the cavern was from.

References

[1]   R. Sturk and H. Stille Design and excavation of rock caverns for fuel storage—cases study from Zimbabwe, Tunnelling and Underground Space Technology, **(1995)**, vol. 10, no. 2, pp. 193-201.
[2]   Y. N. Lee, S. P. Yun and D. Y. Kim, "Design and construction aspects of unlined oil storage caverns in rock", Tunnelling and Underground Space Technology, vol. 11, no. 1, **(1996)**, pp. 33-37.
[3]   Y. N. Lee, Y. H. Suh and D. Y. Kim, "Stress and deformation behaviour of oil storage caverns during excavation", International Journal of Rock Mechanics and Mining Sciences ISRM International Symposium 36th U.S. Rock Mechanics Symposium, vol. 34, no. 3-4, **(1997)**, pp. 301-305.
[4]   X. Gao and Z. Gu, "The application of artificial water curtain to unlined gas storage caverns", Chinese Journal of Rock Mechanics and Engineering, vol. 16, no. 2, **(1997)**, pp. 178-187.
[5]   Z. Zhang, Z. S. Tan, J. Wan and H. Zhang, "Three-dimensional seepage analysis of underground LPG storage with water curtain", Chinese Jounal of Geotechnical Engineering, vol. 25, no. 3, **(2003)**, pp. 331-335.
[6]   W. Chen, W. Li, E. Hou, H. Bai, H. Chai, D. Wang, X. Cui and Q. Wang, "Application of frequency ratio, statistical index and index of entropy models and their comparison in landslide susceptibility mapping for the Baozhong Region of Baoji, China", Arab J Geosci (in press), **(2014)**.
[7]   K. Sarkar, T. N. Singh and A. K. Verma, "A numerical simulation of landslide-prone slope in Himalayan region—a case study", Arab J Geosci, vol. 5, **(2012)**, pp. 73-81.
[8]   T.-H. Yang, W.-H. Shi, P.-T. Wang, H.-L. Liu, Q.-L. Yu and Y. Li, "Numerical simulation on slope stability analysis considering anisotropic properties of layered fractured rocks: a case study", Arab J Geosci (in press), **(2014)**.
[9]   I. Shooshpasha and H. A. Amirdehi, "Evaluating the stability of slope reinforced with one row of free head piles", Arab J Geosci (in press), **(2014)**.
[10] A. Fahimifar, A. Abdolmaleki, P. Soltani, "Stabilization of rock slopes using geogrid boxes", Arab J Geosci, vol. 7, **(2014)**, pp. 609-621.

[11] S. Srikrishnan, J. L. Porathur and H. Agarwal, "Impact of earthquake on mining slopes—a numerical approach", Arab J Geosci (in press), **(2013)**.

[12] Y. Chen, D.-F. Liu, S.-M. Wang and D.-F. Tian, „Factors for stability of three-dimensional unsaturated soil landslides", Chinese Journal of Geotechnical Engineering, vol. 32, **(2010)**, pp. 1236-1240.

[13] E. Topsakal and T. Topal, "Slope stability assessment of a re-activated landslide on the Artvin-Savsat junction of a provincial road in Meydancik", Turkey. Arab J Geosci (in press), **(2014)**.

[14] L. Nie, Z. Li, M. Zhang and L. Xu, "Deformation characteristics and mechanism of the landslide in West Open-Pit Mine", Fushun, China. Turkey. Arab J Geosci (in press), **(2014)**.

[15] X.-H. Xu, Y.-Q. Shang and Y.-C. Wang, "Comprehensive Treatment and Evaluation Decision Method of Gravel Soil Landslide", Journal of Jilin University, vol. 41, **(2011)**, pp. 484-492.

[16] H. Shi, "Stability for Huangdao water seald underground petroleum storage caverns in rock", Beijing Jiaotong University, **(2010)**.

Authors

Yang Shang-Yang, he is a Lecturer of Department of Physics and Mathematics,Shandong Jiaotong University, Jinan,250023,China

Li Shu-Cai, he is a Professor, Director of Geotechnical and Structural Engineering Research Center, Shandong University, Dean of Civil Engineering School, Shandong University, No.17923, Jingshi Rd., Jinan, Shandong, P.R. China.

Xue Yi-Guo, he is a Professor, teacher of Geotechnical and Structural Engineering Research Center, Shandong University, teacher of Civil Engineering School, Shandong University, No.17923, Jingshi Rd., Jinan, Shandong, P.R. China.

Zhang Qing-Song, he is a Professor , teacher of Geotechnical and Structural Engineering Research Center, Shandong University, teacher of Civil Engineering School, Shandong University, No.17923, Jingshi Rd., Jinan, Shandong, P.R. China.